

**ESD RECORD COPY**

RETURN TO  
SCIENTIFIC & TECHNICAL INFORMATION DIVISION  
(ESTI), BUILDING 1211

**ESD ACCESSION LIST**  
ESTI Call No. 59872  
Copy No. 1 of 1 cys.

Technical Note

1967-52

Present Status  
of Cadmium Sulfide  
Thin Film Solar Cells

A. G. Stanley

13 December 1967

Prepared under Electronic Systems Division Contract AF 19(628)-5167 by

**Lincoln Laboratory**

MASSACHUSETTS INSTITUTE OF TECHNOLOGY

Lexington, Massachusetts



ADO 667519

The work reported in this document was performed at Lincoln Laboratory, a center for research operated by Massachusetts Institute of Technology, with the support of the U.S. Air Force under Contract AF 19(628)-5167.

This report may be reproduced to satisfy needs of U.S. Government agencies.

This document has been approved for public release and sale; its distribution is unlimited.

MASSACHUSETTS INSTITUTE OF TECHNOLOGY  
LINCOLN LABORATORY

PRESENT STATUS OF CADMIUM SULFIDE  
THIN FILM SOLAR CELLS

*A. G. STANLEY*

*Group 63*

TECHNICAL NOTE 1967-52

13 DECEMBER 1967

LEXINGTON

MASSACHUSETTS

### ABSTRACT

Cadmium sulfide thin film solar cells, specially selected for stability under ambient conditions, experienced severe degradation in their I-V characteristics when subjected to thermal cycling in vacuum. A number of diagnostic techniques were applied to determine the failure mechanism. These included cross-sectioning, infrared measurements, mechanical stress tests and the measurement of series and shunt resistance. Different types of failure modes are discussed. The results of radiation experiments are summarized.

Accepted for the Air Force  
Franklin C. Hudson  
Chief, Lincoln Laboratory Office

## PRESENT STATUS OF CADMIUM SULFIDE THIN FILM SOLAR CELLS

### I. INTRODUCTION

CdS thin film solar cells have now been under development for a period of 12 years (Ref. 1). Recent improvements in efficiency and environmental stability (Ref. 2-5) suggested that the cells might now be suitable for space applications, where their lower efficiency as compared to silicon might be offset by their ability to form very lightweight self-supporting arrays.

The electrical properties of the CdS thin film solar cells currently produced by Clevite have been fairly well specified (Ref. 1). These properties include the I-V curves, current and power output, effect of illumination intensity, time response, spectral response and the effect of temperature on open circuit voltage, short circuit current and cell efficiency.

The mechanical and environmental behavior of the cells is considerably less well known, because the cells have undergone a number of structural modifications within the last three years listed in Table 1. The last type shown in the Table is the current model. Its structure is shown in Fig. 1. Further details of the construction and mode of operation may be found in Refs. 1 and 2.

In the earlier models most of the problems were due to the pressure contact of the metal grid which was unstable under thermal cycling (Refs. 3,4). Also the nylon (Capran) interlayer caused degradation due to moisture (Ref. 5). The silver epoxy contact avoided these difficulties, but produced a transient drop in output particularly at higher temperatures.

TABLE 1			
Type	Substrate	Metal Grid Contact	Efficiency
1	Metal	Pressure, nylon interlayer	2 per cent
2	Metal	Pressure, nylon interlayer	5 per cent
3	Plastic	Pressure, nylon interlayer	2 per cent
4	Plastic	Pressure, nylon interlayer	4-5 per cent
5	Kapton	Ag Epoxy	4-5 per cent
6	Kapton	Au Epoxy	4-5 per cent

Degradation in thermal cycling remains the major unsolved problem in the development of thin film CdS solar cells. The tests carried out on the latest model, type 6, are therefore described in some detail. A number of diagnostic techniques have been applied to elucidate the failure mechanism. These include cross-sectioning, infrared measurements, mechanical stress tests, and the measurements of series and shunt resistance. The effects of ultraviolet and charged particle radiation are also described.

## II. THERMAL CYCLING

### A. Simulation Requirement

A thin film solar cell array in the synchronous orbit would be subject to extreme temperatures of  $60^{\circ}\text{C}$  (equilibrium value perpendicular to sun at air mass zero) and  $-190^{\circ}\text{C}$  (after 1.2 hours in eclipse). These values are based on calculations by D. Nathanson for two cells mounted back to back, total weight 0.12 lbs/sq. ft.,  $\alpha = \epsilon = 0.9$ . In addition the temperature undergoes a 12 hour cyclical variation from  $60^{\circ}\text{C}$  to a temperature somewhat higher than  $-190^{\circ}\text{C}$  during the rotation of the array with respect to the sun. Each cell will be under slight tension.

Previous vacuum-thermal cycling tests at NASA Lewis Research Center (Ref. 3) and at Boeing (Ref. 6, 7) utilized two test cycles: First, an accelerated short cycle of 15 minutes at  $60^{\circ}\text{C}$ , then 15 minutes at  $-80^{\circ}\text{C}$ ; and second, a longer cycle of 1 hour at  $60^{\circ}\text{C}$ , then 30 minutes at  $-80^{\circ}\text{C}$ . The solar cells were operated under simulated sunlight and all heating and cooling was done by radiation. The longer cycle, which also corresponds more closely to space conditions, is the more severe causing the greater cell degradation. This apparently is due to mechanical stresses set up between layers with different thermal expansion coefficients.

### B. Lincoln Laboratory Tests

All experiments were carried out on cells of the latest design whose structure is shown in Fig. 1. Prior to thermal cycling tests all the cells possessed stable I-V characteristics (to within 0.1%) and had been tested over a period

of 1 month under ambient conditions. They had also been stored in a vacuum oven at  $100^{\circ}\text{C}$  for periods of 24 hours but without application of light. The stability check was introduced in order to screen out units that would fail after a few cycles in thermal vacuum testing.

Several of these cells were subjected to thermal cycling in vacuum between  $60^{\circ}\text{C}$  and  $-190^{\circ}\text{C}$  in the test setup shown in Fig. 2. The test cell was mounted flat on a 4 in. x 4 in. copper plate. During the hot part of the cycle the solar cell was illuminated by one solar constant from a DKW 1000 watt tungsten-halogen lamp. The radiation passed through a heat filter and through a Pyrex window into the vacuum system. The copper plate was cooled to achieve a temperature of  $60^{\circ}\text{C}$  by means of a regulated flow of compressed air through the copper tube supporting it. During the cold part of the cycle liquid nitrogen was circulated through the copper plate and a water cooled shutter in front of the quartz window kept out the light. A complete I-V curve was taken at  $60^{\circ}\text{C}$  at intervals in the course of the experiment. A calibrated silicon solar cell monitored the intensity of the incident light, and the temperature was measured on a platinum resistance thermometer.

Two precautions proved to be very important in obtaining reproducible results. Every part of the cell had to make intimate contact with the copper plate to achieve a uniform temperature over the entire cell. Otherwise parts of the cell would be at a higher temperature leading to changes in the I-V characteristics. Good permanent contact was achieved by means of a silicone rubber with a primer and also with double sticky tape. Also it was necessary to solder separate current and voltage leads directly to the two end contact regions of the cell to avoid changes in contact resistance during thermal cycling.

The results shown in Table 2 indicate that, over the temperature range investigated, the first signs of degradation occur after about 3 days. There was no significant amount of hysteresis in the I-V curves of the degraded cell.

The experimental setup used provides a convenient means of reaching the lowest temperatures to which the cells may be exposed in an array in the synchronous orbit during shadow, but a cell stuck rigidly onto a copper sheet gives a very poor simulation of the thermal and mechanical stresses on the cell forming part of an array without additional backing. Also only one 3 in. x 3 in. cell could be tested at a time, so that longer exposures yielded very little statistically meaningful information.

TABLE 2  
Preliminary Thermal Cycling Experiments at Lincoln Laboratory

Cell Number	3 Hour Cycles	Temperature	Time	$I_{SC}^*$	$V_{OC}^*$	$P_{MAX}^*$
H128BK5	-----	60°C	20 hours	N O C H A N G E		
		190°C	3 hours	"	"	
H125BK6	-----	60°C	6 hours	"	"	
H125BK5	0	90 minutes at 60°C	0	746 mA	0.417V	183 mW
	15	90 minutes at -190°C	46.5 hrs.	745 mA	0.417V	178 mW
	23		71.5 hrs.	741 mA	0.415V	177 mW
	47		142.5 hrs.	720 mA	0.410V	161 mW
*Measured in vacuum at 60°C						

#### C. Boeing Tests

Ten cells from the same batch were sent to be tested in the vacuum-thermal cycling test facility of the Boeing Corporation which had been used for earlier tests on cadmium sulfide thin film solar cells (Ref. 6, 7). The end tabs of the cells were clamped onto an aluminum frame, so that the active area of the cell was not in contact with any material. Nine cells could be tested simultaneously. The arrangement of the cells is shown in Fig. 3. During the hot part of the cycle the cells were illuminated by a Spectrolab X25L solar simulator. The light

intensity at the front surface was set with an airplane calibrated cadmium sulfide solar cell (Cell No. C-11, mylar cover) at  $140 \text{ mW/cm}^2$  AMO. The temperature was measured by means of a copper-constantan thermocouple glued to the center of the rear surface of each cell. The cycle durations and temperature extremes are shown in Table 3. The cells were cycled for a total of 77 cycles over a period of about 1 week. The entire I-V curve was measured at the elevated temperature in vacuum at the end of cycles 1, 37, 60 and 77.

TABLE 3				
Cycle Durations and Cell Temperature Extremes				
Cycle No.	Light Portion		Dark Portion	
	Duration (hours)	Maximum Cell Temperature ( $^{\circ}\text{C}$ )	Duration (hours)	Minimum Cell Temperature ( $^{\circ}\text{C}$ )
1	1	61.5	0.19	-143
2	1	63	2	-128
3-77	1	66	1	-114

Values of short circuit current  $I_{SC}$ , open circuit voltage  $V_{OC}$  and maximum power  $P_{MAX}$  are shown in Table 4. It may be noted that the maximum power of all the cells has degraded at the end of the test by up to 50 per cent. Also, seven of the cells had already degraded at the end of the 37th cycle, whereas the maximum power of the two remaining cells H124CK5 and B935AK degraded by only 15 per cent at the end of the test. These two cells showed the highest fill-factor, i. e. the ratio  $P_{MAX}/V_{OC} \cdot I_{SC}$ , measured before cycling at  $25^{\circ}\text{C}$ . The fill factor may be considered as a figure of merit related to the internal series resistance. The best cells so far constructed possess fill factors between 0.70 and 0.73.

The I-V curves of the degraded cells are unstable and exhibit hysteresis loops such as the one shown in Fig. 4. The cells were severely degraded and remained fairly unchanged from the 37th to the 77th cycle. The short circuit current did not degrade by more than 5 per cent. All these phenomena indicate a delamination rather than a chemical deterioration of the barrier layer.

TABLE 4  
Summary of Boeing Test Results

Cell Number		CYCLES					$P_{MAX} / V_{OC} \cdot I_{SC}$ at 25°C
		0	1	37	60	77	
H-110AK4	$V_{OC}$ (V)	0.411	0.411	0.394	0.386	0.385	0.67
	$I_{SC}$ (mA)	790	790	745	765	750	
	$P_{MAX}$ (mW)	205.3	204	118	124	121.8	
	Temp (°C)	61.5	63	63	66	66	
H-110AK2	$V_{OC}$ (V)	0.407	0.410	0.392	0.372	0.380	0.665
	$I_{SC}$ (mA)	750	750	710	740	710	
	$P_{MAX}$ (mW)	194.6	193	130	119.6	103.2	
	Temp (°C)	60	59	59	62	62	
H-110AK5	$V_{OC}$ (V)	0.403	0.403	0.391	0.388	0.385	0.655
	$I_{SC}$ (mA)	745	745	715	730	715	
	$P_{MAX}$ (mW)	194.6	195	127	122.4	94.5	
	Temp (°C)	60.5	60	61	64	63	
H-124CK5	$V_{OC}$ (V)	0.403	0.403	0.406	0.394	0.390	0.69
	$I_{SC}$ (mA)	750	765	760	780	760	
	$P_{MAX}$ (mW)	185.4	188	188	174	157.1	
	Temp (°C)	61	61	58	61	59	
H-106BK5	$V_{OC}$ (V)	0.401	0.403	0.386	0.387	0.374	0.66
	$I_{SC}$ (mA)	800	810	780	800	770	
	$P_{MAX}$ (mW)	184.6	184	138	152.3	126.4	
	Temp (°C)	62.5	63	62	64	64	
B-935AK	$V_{OC}$ (V)	0.399	0.397	0.402	0.394	0.393	0.71
	$I_{SC}$ (mA)	780	780	770	780	770	
	$P_{MAX}$ (mW)	194.8	195	189	176.6	165.2	
	Temp (°C)	62.5	63	62	66	64	
H-108BK8	$V_{OC}$ (V)	0.411	0.413	0.389	0.384	0.380	0.66
	$I_{SC}$ (mA)	735	735	710	730	720	
	$P_{MAX}$ (mW)	193.0	194	99	111.5	117.5	
	Temp (°C)	60	58	57	58	58	

TABLE 4 (Cont)							
Cell Number		CYCLES					$\frac{P_{MAX}}{V_{OC} \cdot I_{SC}}$ at 25°C
		0	1	37	60	77	
H-99AK5	$V_{OC}$ (V)	0.412	0.410	0.388	0.386	0.388	0.67
	$I_{SC}$ (mA)	760	780	760	770	760	
	$P_{MAX}$ (mW)	185.6	183	122	122.4	121.8	
	Temp (°C)	60.5	62	61	64	63	
H-110AK6	$V_{OC}$ (V)	0.412	0.403	0.388	0.385	0.382	0.68
	$I_{SC}$ (mA)	765	770	730	740	740	
	$P_{MAX}$ (mW)	197.8	181	129	108.8	117.0	
	Temp (°C)	52	62	48	52	49	

It has been suggested that the solar cells might be damaged if they are cycled while stretched onto an aluminum frame due to the difference between the expansion coefficients of aluminum and cadmium sulfide. This possibility is discussed in Section VII. Fig. 3 shows that the suspension of the cells is quite slack.

There is a systematic error in the Boeing measurements of the I-V characteristics which reduces the open circuit voltage by 40 mV and the short circuit current by about 7 per cent at 25°C. This has been traced to a circuit fault. The original measurements at Clevite have been confirmed at Table Mountain. These values have been corrected for air mass zero for comparison with the Boeing results.

The lowest temperature achieved during the cold portion of the cycle was far too high for adequate simulation of the space environment. It is not believed, however, that lower temperatures would have resulted in even further degradation.

#### D. Thermal Cycling Facilities Under Development

Although the results at Lincoln Laboratory and at Boeing are in qualitative agreement, the absence of severe hysteresis loops indicates that a cell stuck

rigidly onto a cold wall provides a poor simulation of the space environment. Two new thermal cycling systems are therefore being developed here. In a small system capable of holding only 4 cells, the cells will be surrounded by a copper shroud inside a vacuum bell jar through which liquid nitrogen is circulated. Heat and illumination are provided by a tungsten-halide lamp. A large system with a maximum available area of 4 ft. x 4 ft. makes use of the 78 inch environmental chamber of the Lincoln Accelerator Laboratory. A 20 kw Xenon lamp is used for measurement purposes only. In the absence of the illumination heat will be provided from a nichrome resistance heater mounted directly behind the test cells which will be withdrawn during the cold portion of the cycle. In both systems the cells will be freely suspended and tensioned by known weights. The two systems will make it possible to compare the effects of heat alone with the combined effect of heat and current generated by illuminating the cell.

### III. CROSS-SECTIONING

A number of cells have been cross-sectioned at right angles to the plane of the cell and photomicrographs obtained at 400 X magnification. Practically all of these reveal defects which could lead to degradation under thermal cycling. Some typical photos are shown in Figs. 5-7. The defects fall in the following categories:

#### A. Gold-Epoxy Bond

The gold-epoxy bond between the  $\text{Cu}_2\text{S}$  barrier layer and the gold-plated grid is completely or partially missing (Fig. 5) or displaced (Fig. 6). In all cells examined, even those with fill factor greater than 0.7, few points of contact between the grid and barrier layer are visible. It is evident that the contacts are sufficient to produce good I-V characteristics. It has been shown that good initial characteristics are obtained even if the gold epoxy is completely absent. It is suspected that the contacts are too weak to withstand thermal cycling causing delamination over certain regions of the cell.

### B. Bond Between Ag-Polyimide, Zinc and CdS Layers

This bond delaminates in some areas (Fig. 6, 7). The failure mode has only occasionally been observed. It cannot be established from the photographs if the CdS detaches from either the silver layer or from the zinc plating.

### C. Cracks in the CdS

Vertical cracks through the CdS layer shown in Fig. 5 are very common. They are associated with differential expansion of the CdS and the Kapton during lamination or other parts of the fabrication process where heat is applied. A more complete fracture of the CdS, such as shown in Fig. 7 is rare. All defects described so far were observed before thermal cycling. A detailed study was made of 3 CdS thin film solar cells which had experienced severe degradation under thermal cycling at the Boeing Test Facility. Infrared tests at the Barnes Engineering Company revealed hot spots indicating a very uneven current distribution (see below).

Four different regions of each cell were then cross-sectioned. Most of the cross-sections showed extended lateral cracks in the cadmium sulfide layer such as shown in Fig. 8. Similar cracks had not been detected in cross-sections of cells not subjected to thermal cycling. In several cross-sections the cracks extended laterally from the grid contact indicating maximum stress under the latter.

A dilute solution of KCN was able to dissolve the region above the cracks in one of the degraded cells which were located about  $5\mu$  from the grid contact. There appears to be some uncertainty about the location of the  $\text{Cu}_2\text{S}$ -CdS interface. Shirland (Ref. 1) states that the  $\text{Cu}_2\text{S}$  layer is only  $1000 \text{ \AA}$  thick. Shiozawa et al. (Ref. 14) obtained a thickness of  $0.59\mu$  for the  $\text{Cu}_2\text{S}$  layer on CdS evaporated on a Pyrex substrate by dissolving it in a dilute KCN solution. However, this structure differs from that of a regular solar cell in the substrate material and also is not subjected to the subsequent heat treatments described in Section VII. At higher temperatures copper ions in the barrier

layer diffuse further into the cadmium sulfide. This widens the barrier layer and should therefore result in changes of the spectral response of the cell.

The photomicrographs also show up other defects such as window areas covered with gold epoxy or small voids in the clear epoxy.

#### IV. INFRARED MEASUREMENTS

The potentialities of applying infrared measuring techniques to thin film solar cells were investigated with the assistance of the Barnes Engineering Company. An infrared camera was used to obtain a thermogram of the solar cell, whose detailed structure was then examined under an infrared microscope.

If the bottom of the solar cell makes good thermal contact with a metal plate, the surface temperature is very uniform even if heat is applied to the metal plate or if current is passed through the cell. This is undoubtedly due to the excellent thermal conductivity of cadmium sulfide (see Table 7).

On suspending the cell from a frame in air and passing currents of 0.5 amp to 1 amp in the forward direction (applied voltage less than 1V) the temperature distribution in degraded cells viewed from the front becomes very uneven and hot spots of 1/4 in. to 1 in. diameter are formed. The hot spots can reach temperatures as high as 135°C in air while the cold regions remain near ambient. In vacuum even higher temperatures will be obtained. The infrared microscope did not reveal any fine structure within the hot regions. The peak temperature extended over a distance of only 3 mils coinciding with one of the grid lines. The location of the hot spots varied from one cell to the next. The temperature of the hot spots oscillated by as much as 30°C in some samples with a period of the order of 30 seconds.

These phenomena suggest a delamination between conducting layers in the cold regions resulting in intermittent electrical contacts subject to mechanical stresses that vary with temperature. In at least one instance passing 0.5 amps in the forward or reverse direction resulted in the same hot spot temperature. This may have been due to localized short circuit paths even though the cell as a whole still showed normal rectification.

Before thermal cycling the cells were fairly uniform in temperature, within  $1.5^{\circ}\text{C}$ . An experimental cell without any gold epoxy bonding between the grid and the  $\text{Cu}_2\text{S}$  layer showed severe hot spots (see Fig. 9) although its I-V characteristics were indistinguishable from any other cell before cycling.

The infrared technique appears to be a very promising method for investigating the current and temperature distributions in thin film solar cells. Of course, the current must be supplied externally, since photovoltaic generation would swamp the sensitive thermistor detectors.

## V. MECHANICAL STRESS TESTS

A few cells were subjected to an 'Instron' tension test. The samples were cemented with epoxy polyamide to two gold plated brass cylinders of  $1\frac{1}{8}$  in. diameter. A tension of 1700 psi normal to the cell surface produced delamination between the silver-polyimide layer and the zinc plating in some areas and between the cadmium sulfide and the zinc plating in others. The delaminated surface was then cemented once more to a clean brass cylinder. A break within the cadmium sulfide layer was caused by a renewed tension of 1500 psi.

Several regions of a cell which had been severely degraded after thermal cycling were cemented with epoxy between two mating  $\frac{1}{2}$  inch diameter aluminum cylinders. After curing, the cylinders were pulled apart in the Instron tensile tester. There were two types of failure planes. One was in the Zn-Ag polyimide interface and the other in the  $\text{Cu}_2\text{S}$  layer. These were readily distinguishable as distinct plateaus under 40 x stereo microscope magnification. The microscopic examination of the fractured  $\text{Cu}_2\text{S}$  layer revealed a dark, dense, metallic region readily soluble in dilute KCN near the grid and a thin dark coating not as soluble in dilute KCN which covered the brownish red CdS. This indicates that the  $\text{Cu}_2\text{S}$  layer consists of at least two different compounds with different chemical properties.

Four samples were tensile tested with the results shown in Table 5.

TABLE 5			
Tensile Strength Tests			
Sample	Failure Area (per cent)		Tensile Strength (psi)
	Ag-Zn Layer	Cu <sub>2</sub> S Layer	
A	98	2	1910
B	90	10	1300
C	50	50	1820
D	50	50	1310

A peel test was applied to some specimens. A peak force of 0.7 lbs per inch of width caused the bottom Kapton layer to delaminate from the silver-polyimide layer.

## VI. SERIES RESISTANCE AND SHUNT RESISTANCE

The measurement of series and shunt resistance of cadmium sulfide solar cells under illumination are described by Brandhurst and Hart (Ref. 8). The principles are illustrated in Fig. 10. The shunt resistance is measured by applying the method of Wolf and Rauschenbach (Ref. 9). I-V curves are generated at two different intensities of illumination  $L_1$  and  $L_2$ , and an arbitrary point  $(I_1, V_1)$  near the maximum power point on the highest curve is selected. A point  $(I_2, V_2)$  is located on curve  $L_2$  such that  $I_{SC1} - I_1 = I_{SC2} - I_2$ . The series resistance  $R_S$  is then given by

$$R_S = \frac{\Delta V}{\Delta I} = \frac{V_2 - V_1}{I_{SC1} - I_{SC2}} \quad (1)$$

The derivation of this relationship is based on the equation (Ref. 10)

$$I = I_0 \left\{ \exp \frac{q}{AkT} (V - I R_S) \right\} - I_L \quad (2)$$

where the shunt resistance has been neglected.  $I$  and  $V$  denote the terminal current and voltage.  $A$  is a constant of order 1, and  $I_0$  represents the reverse diode saturation current. The following additional assumptions are made in the derivation of (1):

1. The light generated current  $I_2$  is proportional to the incident light intensity, but independent of the current-voltage characteristics.

2.  $R_S$  is a constant, independent of the light level and of the point along the I-V curve.

Some experiments were performed to test the validity of these assumptions for 3 in. x 3 in. cadmium sulfide thin film cells.  $R_S$  is made up of contact resistances between the semiconductor and the metallized layers, the sheet resistance in the  $\text{Cu}_2\text{S}$  layer and the bulk resistance in the CdS. The resistance of the gold plated copper grid may be neglected (approximately 5 milliohm). Fig. 11 shows that the series resistance varies linearly with the voltage. Since this is a fairly large effect, it is important to define a position on the I-V curve when comparing  $R_S$  of different devices. The maximum power point has been used for all subsequent measurements. The irradiance of the lower illumination level  $L_2$  was then varied keeping the irradiance  $L_1$  constant at  $140 \text{ mW/cm}^2$ . Fig. 12 shows that the effect on  $R_S$  is less than 10 per cent as long as the irradiance of the lower light level is greater than  $70 \text{ mW/cm}^2$ . The ratio  $L_1/L_2$  was kept at about 0.75 in subsequent measurements. Fig. 13 shows  $R_S$  as a function of the irradiance  $L_1$ . The photoconductive property of cadmium sulfide causes  $R_S$  to decrease sharply with  $L_1$  initially. Beyond  $150 \text{ mW/cm}^2$  the curve flattens out. The Figure also shows  $R_{OC}$ , the series resistance obtained from the slope of the I-V curve  $L_1$  at the open circuit voltage  $V_{OC}$  (see Fig. 10). The measurement of  $R_{OC}$  is less accurate than that of  $R_S$  and yields somewhat lower resistance values.

The shunt resistance  $R_{SH}$  was obtained from the slope of the I-V curve for negative voltages shown in Fig. 10. It also decreases as the intensity of

illumination is increased. The values of  $R_{SH}$  shown in Table 6 are extremely low. 1 x 2 cm cells have a shunt resistance of about 600 ohms (Ref. 8) at one solar constant. The manufacturer states that a larger number of short-circuit paths in the 3 in. x 3 in. cell are responsible for the reduction in  $R_{SH}$  over and above the geometrical scale factor.

Table 6 indicates that the series resistance of the 3 in. x 3 in. cells before cycling varies over a wide range, presumably reflecting the quality of the contacts. This parameter is not at present measured for all cells, so that typical production limits are not available. The cell degraded in thermal cycling goes through a minimum at one solar constant suggesting a restriction in the current path at high current levels.

TABLE 6					
Irradiance mW/cm <sup>2</sup>	H126BK4 before cycling		H126AK1 before cycling	H126BK5 before cycling	
	$R_S$ ohms	$R_{SH}$ ohms	$R_S$ ohms	$R_S$ ohms	$R_{SH}$ ohms
280	0.12	5.0	0.08	0.18	5.7
140	0.26	8.3	0.11	0.09	10.6
70	0.58	12.9	0.22	0.23	17.4
35		23.5	0.35		42.2

## VII. FAILURE MECHANISMS

### A. Thermal Stresses

The failure mechanisms responsible for cell degradation under thermal cycling may be broadly divided into thermal stresses causing contact delamination and chemical changes in the  $Cu_2S$  barrier layer. While chemical effects cannot be ruled out, the catastrophic failure after 37 cycles followed by little damage on further cycling which 7 out of 9 cells experienced in the Boeing test would indicate that thermal stresses constitute the predominant failure mode.

Further evidence may be derived from the unstable I-V curves showing hysteresis effects and from the infrared measurements.

It may be seen from Table 7 that there is a severe mismatch in the thermal expansion coefficients of CdS ( $6.5 \times 10^{-6}/^{\circ}\text{C}$  parallel to substrate) and those of the other constituents of the solar cell. The CdS is deposited at a temperature of  $220^{\circ}\text{C}$  onto the substrate consisting of layers 1-3, Fig. 1, which is free to expand or contract laterally, but which is prevented from bending. The composite CdS-Kapton film is under severe stress on cooling to ambient, and the film will curl up into a cylinder of 1/4 in. diameter if all constraints are removed. In the subsequent fabrication process the temperature of the cell is raised once to  $250^{\circ}\text{C}$  and two times to  $196^{\circ}\text{C}$ .

TABLE 7				
Thermal Properties				
Material	Coeff. of Linear Thermal Expansion		Thermal Conductivity watts/cm <sup>2</sup> K	Reference
	$10^{-6}/^{\circ}\text{C}$	Temp. or Temp. Range		
CdS single crystal    to axis	4.0	$40^{\circ}\text{C}$	10	11
CdS single crystal ⊥ to axis	6.5	$40^{\circ}\text{C}$		
H film, Kapton	20	- 14 to $38^{\circ}\text{C}$	$1.6 \times 10^{-3}$	12
Copper, tough pitch	16.8	$27^{\circ}\text{C}$	3.9	11
Aluminum	23.2	$27^{\circ}\text{C}$	2.2	11
Molybdenum	5.0	$27^{\circ}\text{C}$	1.4	11

In the lamination process the cell is heated to  $196^{\circ}\text{C}$  at 100 psi for 10 minutes. If the cell is clamped to an aluminum plate during this process,

vertical cracks of the type shown in Fig. 5 develop in the CdS, whereas no cracks appear if the cell is free to expand laterally. This may be due to thermal shock, or else it could be that the stresses present immediately after deposition of the CdS have been relaxed. This assumption is based on the fact that Kapton and aluminum possess comparable expansion coefficients. It is important to note that neither the cracks in the CdS nor the lamination process have any significant effect on the I-V curve of the cell prior to vacuum-thermal cycling.

#### 1. Contact Delamination

There is at present no clear evidence pointing to either the top or bottom contacts as the seat of delamination. A bad thermal mismatch exists in both areas. Cross-sectioning shows that the grid makes electrical contact to the barrier layer at relatively few places. The strength of the gold epoxy bond is difficult to test, as it is likely to be affected by the subsequent application and curing of the clear epoxy. The latter provides a very strong bond between the top Kapton layer and the barrier layer and penetrates into the voids underneath the grid. The clear epoxy possesses a shear strength of 2000 psi at room temperature, but at 100°C this is reduced to only 150 psi.

Delamination at the bottom contact is only rarely seen in cross-sections, but the Ag-polyimide-Zn-CdS interface is one of the failure planes in tensile tests.

#### 2. Lateral Cracks in Semiconductor

In some cells the copper ions appear to have diffused about 5 $\mu$  into the CdS and rupture occurs after thermal cycling due to stresses in this weak region. There is no evidence to show that the fracture line actually corresponds to a distinct CdS - Cu<sub>2</sub>S interface. The recent review by Cook (Ref. 15) shows that the phase structure near the interface may be very complex indeed.

It may be helpful to review two similar displacement processes in the electroplating field that produce notoriously poor bonds. If an iron nail is

dipped into an acid sulfate solution, a beautiful copper coating results which can readily be thumbnailed off. Additionally in Ag plating, copper displacement reactions are avoided by striking in a dilute Ag solution, otherwise a blistered deposit will result.

#### B. Chemical Changes

The  $\text{Cu}_2\text{S}$  barrier layer is extremely sensitive to chemical reactions and diffusion processes which change the concentration or nature of its constituents. The application of heat alone causes three different types of degradation which have to be separated in any experimental investigation.

a. Work at NASA Lewis Research Center has shown that solar cells degrade when illuminated by one sun at  $60^\circ\text{C}$  in vacuum for periods of several days or more. The cells recover on standing in air at ambient. Delamination is suspected as the cause.

b. Cells degrade rapidly when heated below  $100^\circ\text{C}$  in air or oxygen (Ref. 13). The oxygen acts as an acceptor in the  $\text{Cu}_2\text{S}$  layer reducing its resistance. Traces of oxygen may have the same effect.

c. Cells of the current construction, type 6, Table 1, degrade fairly rapidly when heated in vacuum at  $150^\circ\text{C}$  and more slowly at  $100^\circ\text{C}$  (Ref. 2). Individual cells of earlier types were stable at  $100^\circ\text{C}$  for periods up to 8 months. The degradation is believed to be primarily due to delamination, but chemical changes or diffusion processes may be contributing causes.

Copper, nickel, silver, aluminum, palladium and other metals in contact with the barrier layer cause degradation. The copper reacts with the p-type cuprous sulfide layer converting it to cupric sulfide (Ref. 16). It is for this reason that the copper grid is electroplated with gold. The plating is very thin and may provide an insufficient barrier in places. The reaction with copper and nickel lowers the open circuit voltage.

Both the clear and the gold epoxy can contribute to cell degradation in the following ways:

- a. Incomplete curing of the epoxy;
- b. Chemical reactions of impurities in the epoxy with the barrier layer;
- c. Gas evolution from the epoxy;
- d. A chemical reaction between the epoxy and copper in the barrier layer.

The epoxy bond seems to be very effective against degradation due to moisture (Ref. 4, 5).

Chemical reactions at the bottom contact are possible, resulting in:

- a. Increased rectification at the ohmic CdS-Zn-Ag polyimide contact;
- b. Increased series resistance in the Ag-polyimide layer which may be quite non-uniform;

All the processes discussed above possess a definite activation energy and should increase exponentially with temperature. More long term steady state experiments are needed to determine degradation as a function of temperature and time. Chemical degradation will ultimately occur in hot spots produced by uneven current flow after delamination in vacuum thermal cycling.

## VIII. EFFECTS OF CHARGED PARTICLES AND ULTRAVIOLET RADIATION

An extensive study of the effect of electron and proton irradiation on type 3 and 4 solar cells was made at NASA Lewis Research Center (Ref. 8). The output was unaffected by 2.5, 1.0 and 0.6 MeV electrons up to a total dose of  $10^{16}$  e/cm<sup>2</sup>, the maximum dose for the more efficient cells, type 4. Cells encapsulated in Mylar showed considerable embrittlement at higher doses. The low efficiency cells, type 3, were also irradiated with 10, 7, 5 and 2 MeV protons. At a total dose of  $10^{12}$  p/cm<sup>2</sup>, there was a 5 per cent loss in power.

Loferski of Brown University irradiated some early naked cells on a plastic substrate (type 4), i. e. without any front cover, with electrons in the

range from 150 to 500 keV. No change in output or spectral response was observed at total doses up to  $10^{18}$  e/cm<sup>2</sup> at an energy of 425 keV.

Loferski has criticized the lack of energy dependence of the proton damage in thin film solar cells (Ref. 17). Bare 5-6 per cent efficient thin film CdS solar cells manufactured by RCA were subjected to radiation by 50, 100 and 400 keV protons at flux levels of  $10^{12}$  to  $10^{15}$  p/cm<sup>2</sup>. Hui and Corra (Ref. 18) showed that the damage went through a maximum at 100 keV resulting in degradation of short circuit current by 20 per cent at a total dose of  $10^{13}$  e/cm<sup>2</sup> as well as in a considerable reduction in open circuit voltage. A protective silicone coating gave complete protection up to 400 keV (Ref. 19). Unfortunately, similar measurements on Cleveite cells have not been made.

The devices have been subjected to UV tests at NASA Lewis Research Center. UV has no effect on Kapton cells, but Mylar cells are severely embrittled. A thin layer of polyimide is sufficient to protect Mylar cells (Ref. 2).

## X. CONCLUSIONS

The power output of cadmium sulfide thin film solar cells as presently constructed will degrade as much as 50 per cent when freely suspended in a space environment due to thermal cycling between 60°C and low temperatures in the range from -110 to -190°C. The basic cause of the degradation is the severe mismatch in the thermal expansion coefficients between the cadmium sulfide layer and the other layers making up the cell which produces delamination at either the top or bottom electrical contacts to the semiconductor layer or fractures within the semiconductor material.

During fabrication the cell undergoes several severe heating cycles which greatly complicate a stress analysis of the final product. In addition a number of reversible and irreversible chemical changes take place at elevated temperatures. The multiplicity of factors limit the usefulness of more detailed analytical and diagnostic techniques applied to the existing structure.

It is therefore more fruitful to introduce carefully controlled changes in the structure of the cell and to subject the experimental cells to both thermal

cycling and steady state temperature stress in vacuum. The changes should include modifications of both top and bottom contacts as well as changes in the materials in contact with the barrier layer.

There is strong evidence that thermal cycling may cause extended lateral fractures within the semiconductor itself. Even if this failure mechanism is correct, the grid still plays a very important role since it provides a mechanical constraint for the  $\text{Cu}_2\text{S}$  layer. An electroplated grid a few microns thick offers far less constraint than the gold plated copper grid of the present structure. A few experimental devices of this type survived 6,500 cycles of thermal cycling before degradation set in (Ref. 6). The epoxy bond to the top Kapton layer must also be taken into account.

## ACKNOWLEDGEMENT

The author wishes to acknowledge the assistance of L. P. Farnsworth and E. Murphy in many of the experimental investigations described in this Technical Note.

## REFERENCES

1. F. A. Shirland, "The History, Design, Fabrication and Performance of CdS Thin Film Solar Cells," *Advanced Energy Conversion* 6, pp. 201-222 (1966).
2. J. R. Hietanen and F. A. Shirland, "The Status of the Clevite CdS Thin Film Solar Cell," *Conference Record of the Sixth Photovoltaics Specialists Conference, Cocoa Beach, Florida (28-30 March 1967)*, pp. 179-187.
3. A. E. Spakowski and J. G. Ewashinka, "Thermal Cycling of Thin-Film Cadmium Sulfide Solar Cells," *NASA TND-3556* (1966).
4. A. E. Spakowski, "Some Problems of the Thin-Film Cadmium-Sulfide Solar Cell," *IEEE Trans. Electronic Devices* ED-14, No. 1 (January 1967), pp. 18-21.
5. A. E. Spakowski, et al., "Effect of Moisture on Cadmium Sulfide Solar Cells," *NASA TND-3663* (October 1966).
6. A. E. Spakowski and K. L. Kennerud, "Environmental Testing of Thin Film Solar Cells," *Conference Record of the Sixth Photovoltaic Specialists Conference, Cocoa Beach, Florida (28-30 March 1967)*, I, pp. 201-209.
7. K. L. Kennerud, "Space Environment Tests on Thin Film Solar Cells," *NASA Contract NAS 3-6008 Topical Report, A Summary of Work Completed in Phase I and II, 25 July 1964-30 January 1967 (22 February 1967)*.
8. H. W. Brandhurst and R. E. Hart, "Radiation Damage to Cadmium Sulfide Solar Cells," *NASA Technical Note, NASA TN D-2932* (July 1965).
9. M. Wolf and H. Rauschenbach, "Series Resistance Effects on Solar Cell Measurements," *Advanced Energy Conversion* 3, pp. 455-479 (1963).
10. M. B. Prince, "Silicon Solar Energy Converters," *J. Appl. Phys.* 26, No. 5 (May 1955), pp. 534-540.
11. American Institute of Physics Handbook, 2nd Edition (1963) McGraw Hill.
12. DuPont Kaplon Polyimide Film Bulletin H-2, E. I. DuPont de Nemours and Company (Inc.) Film Department, Wilmington, Delaware.
13. E. R. Hill, B. G. Keramidas and D. J. Krus, "Further Considerations on the Model for the CdS Solar Cell," *Conference Record of the Sixth Photovoltaic Specialists Conference, Cocoa Beach, Florida (28-30 March 1967)*, I, pp. 35-50.

14. L. R. Shiozawa, et al. "Research of the Mechanism of the Photovoltaic Effect in High-Efficiency CdS Thin Film Solar Cells," Interim Technical Report on Contract AF33(615)-5224, Clevite Corporation, July 1967.
15. L. R. Shiozawa, et al. "Research on the Mechanism of the Photovoltaic Effect in High-Efficiency CdS Thin Film Solar Cells," Fifth Quarterly Progress Report on Contract AF33(615)-5224, Clevite Corporation, October 27, 1967.
16. J. C. Schaefer, J. Evans and T. A. Griffin, "Development of Cadmium Sulfide Photovoltaic Film Cell," Harshaw Chemical Co., Final Report on Contract NAS 3-8515 (October 1967).
17. J. J. Loferski, "The Effects of Electron and Proton Irradiation on Thin Film Solar Cells," Revue de Physique Appliquee 1 (September 1966), pp. 221-227.
18. W. L. C. Hui and J. P. Corra, "Thin-Film Cadmium Sulfide Solar Cell Array on Plastic Substrate," Proc. of the Fifth Photovoltaic Specialists Conference (October 1965).
19. G. J. Brucker, et al. "Low Energy Proton Irradiation of Coated and Uncoated Thin-Film CdS and Single-Crystal Si Solar Cells," Proc. IEEE (June 1966), pp. 895-896.

# DESCRIPTION OF FIGURE 1

1. Nominal array cell area =  $2.93 \times 3.25 = 9.52$  sq. in. or 0.0661 sq. ft.
2. Minimum active cell area =  $2.82 \times 3.25 = 8.065$  sq. in. or 0.0560 sq. ft.
3. Nominal closed area of grid = 19.6%.
4. Overall thickness = 0.004 in.
5. Adhesive "A" between layers 5 and 6 is a conducting epoxy.
6. Adhesive "B" between layers 6 and 7 and 5 and 7 is clear epoxy transparent to sunlight.
7. Individual solar cell weight is  $2.36 \times 10^{-3}$  pounds (1.608 grams).
8. Internal cell construction taken from Refs. 1 and 2.

## 9. Construction of solar cell

Layer No.	Material	Thickness
1	Kapton, polyimide, H film	0.001 in.
2	Ag + polyimide varnish, 50% Ag by volume	0.0003 in.
3	Zinc plating	
4	CdS film, vacuum deposited fiber axis orientation - C axis perp. to substrate	0.0006 to 0.001
5	P-type $\text{Cu}_2\text{S}$ layer	
6	Au plated Cu grid	0.00045 in.
7	Kapton, polyimide, H film	0.001 in.
8	Kapton, polyimide, H film	0.0005 in.
9	Gold plating	
10. Grid:	169 openings in width 29 openings in length 4901 openings total	

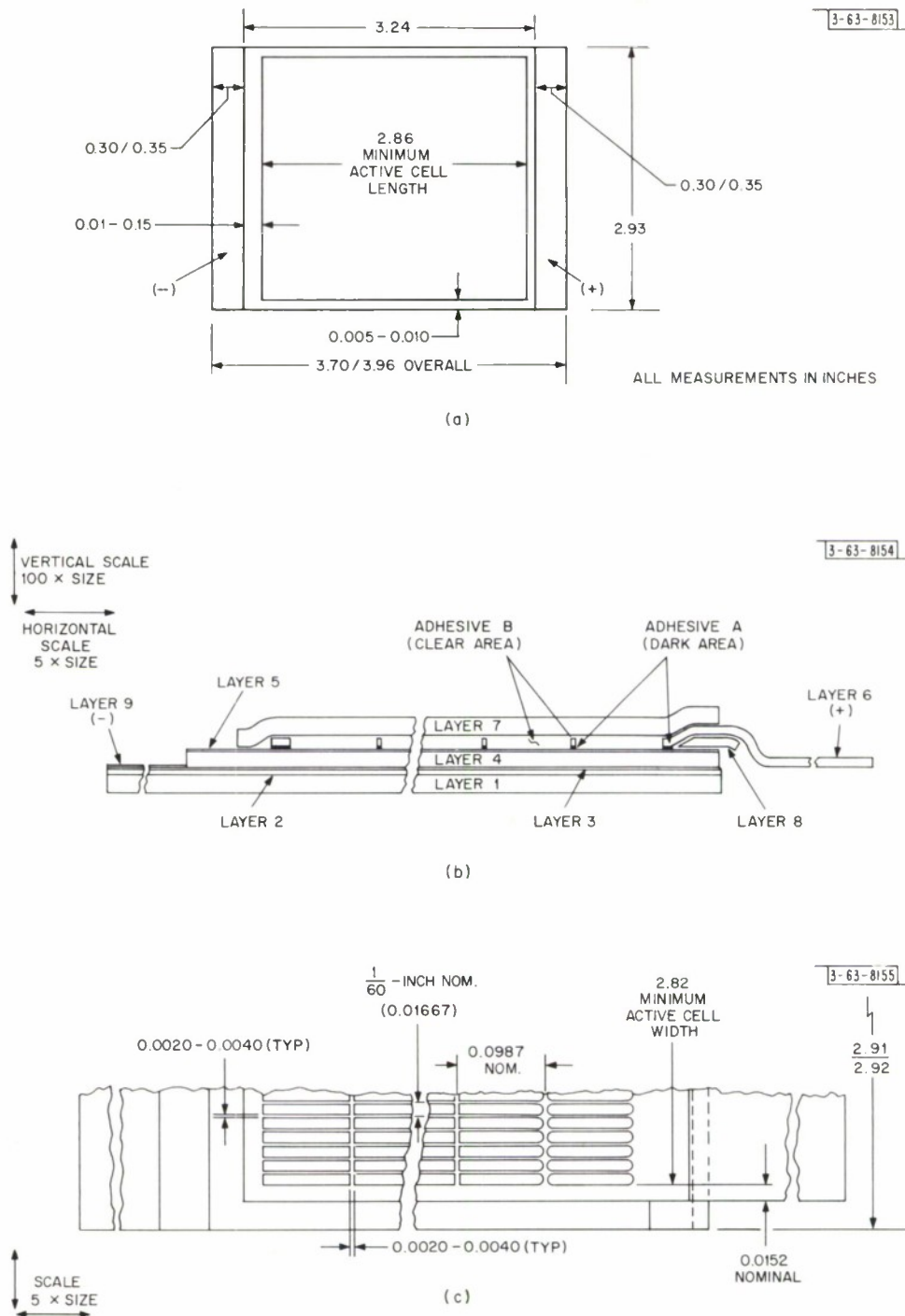


Fig. 1. Construction of cadmium sulfide thin film solar cell.  
 (a) Overall cell dimensions. (b) Vertical cross-section through cell (cut through X axis). (c) Grid layer 6.

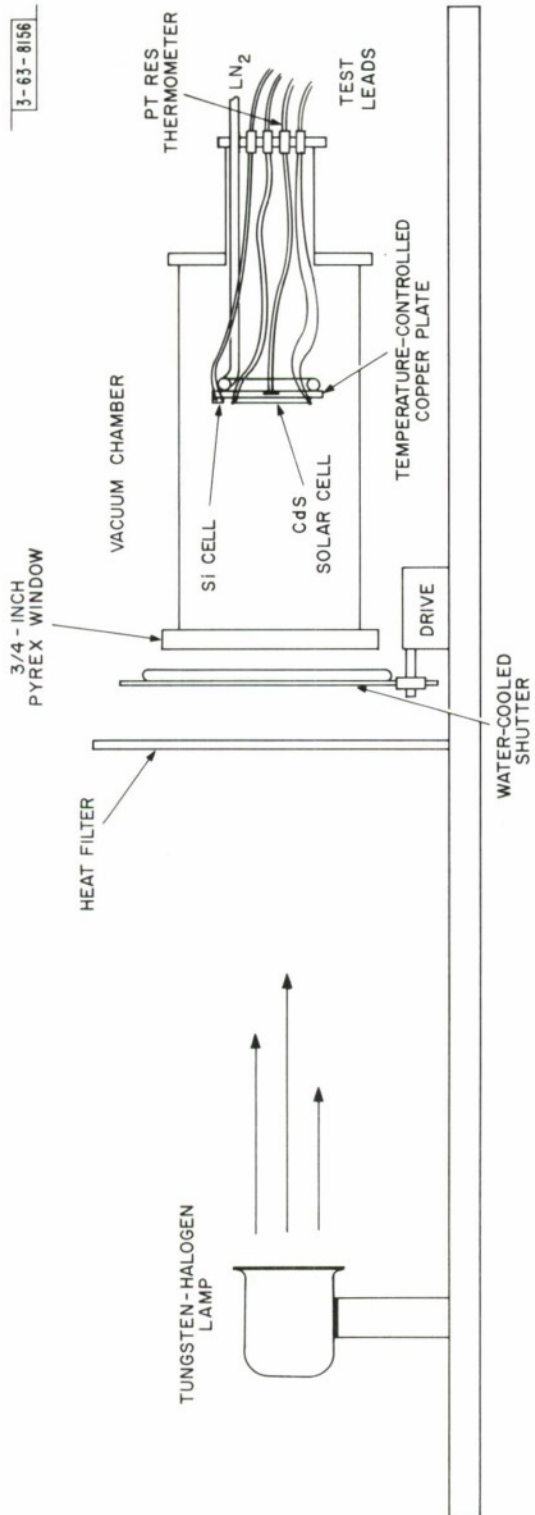
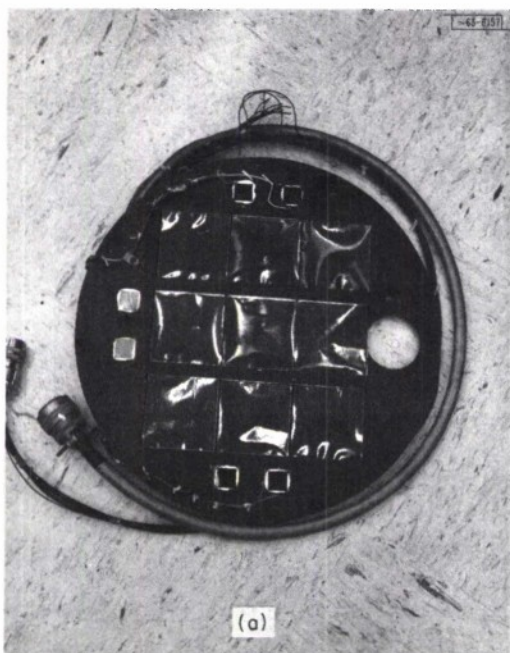
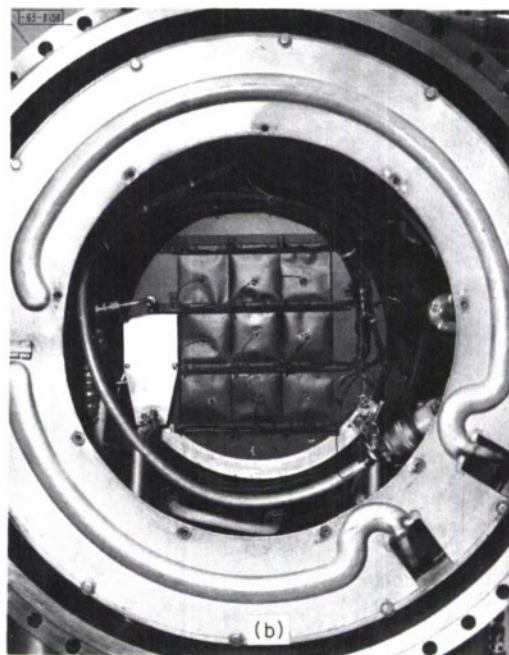


Fig. 2. Thermal vacuum cycling setup.



(a) Front.



(b) Rear.

Fig. 3. Cell assembly in Boeing facility.

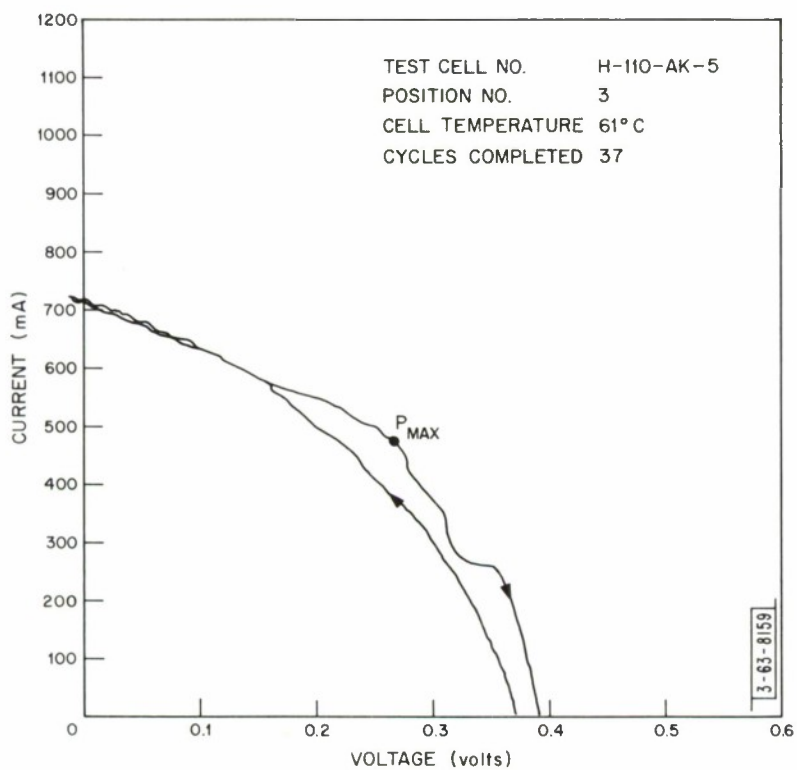


Fig. 4. I-V characteristics of a degraded cadmium sulfide thin-film solar cell.

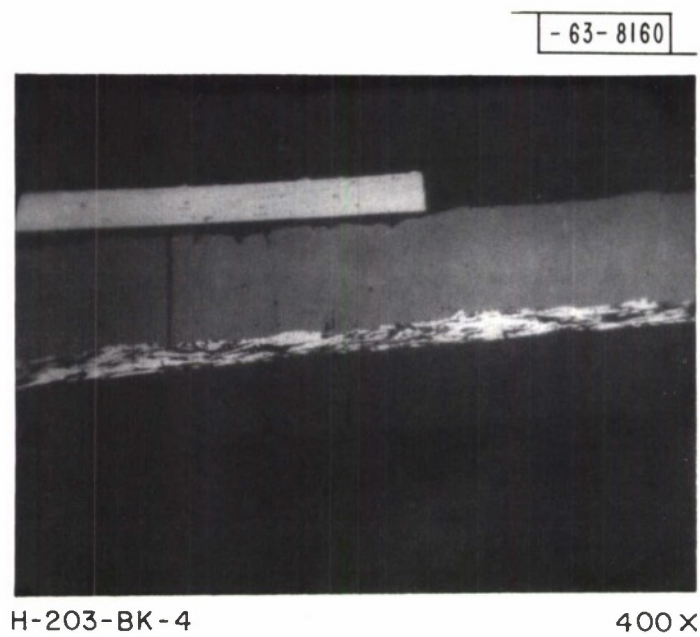


Fig. 5. Photomicrograph of cross-sectioned solar cell.

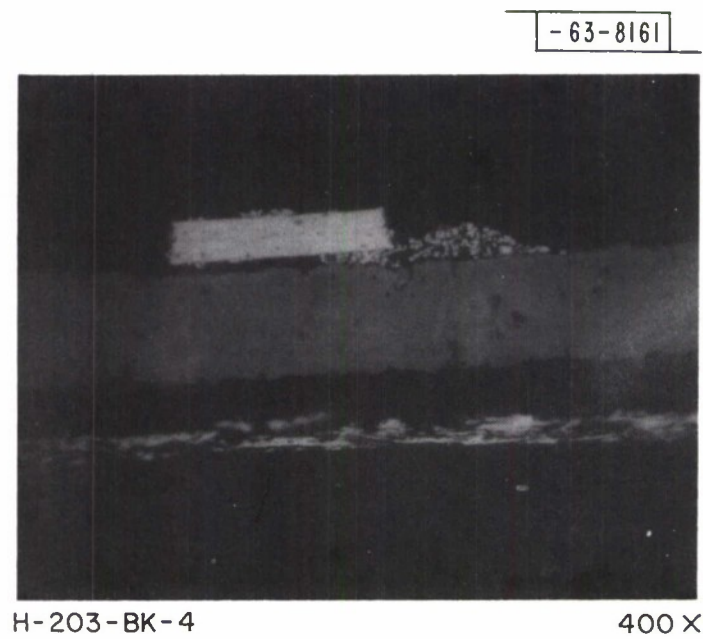


Fig. 6. Photomicrograph of cross-sectioned solar cell.

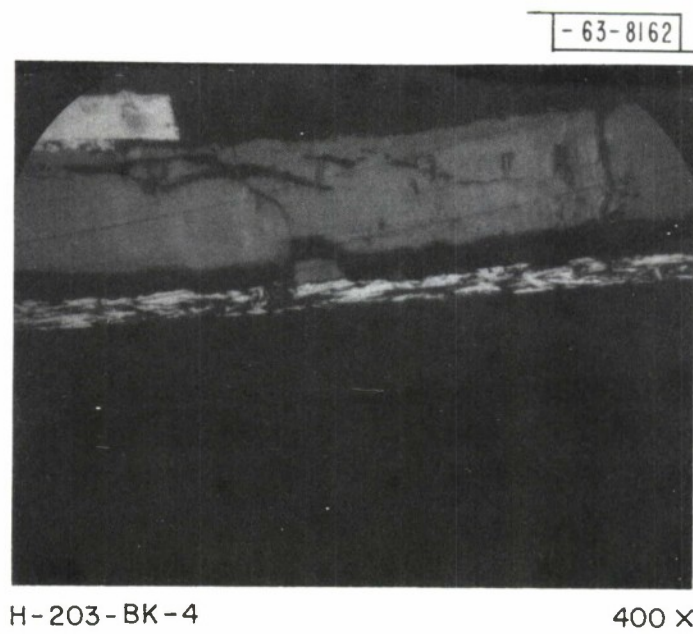


Fig. 7. Photomicrograph of cross-sectioned solar cell.

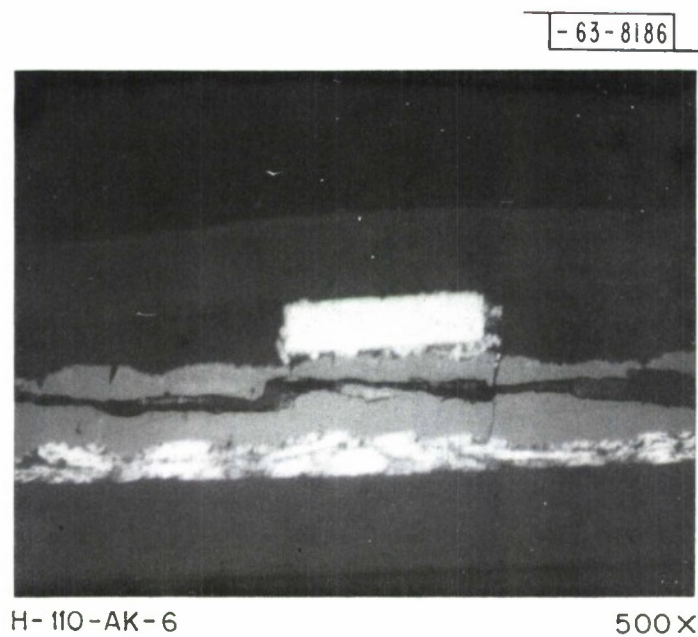


Fig. 8. Cross-section of solar cell degraded in thermal cycling.

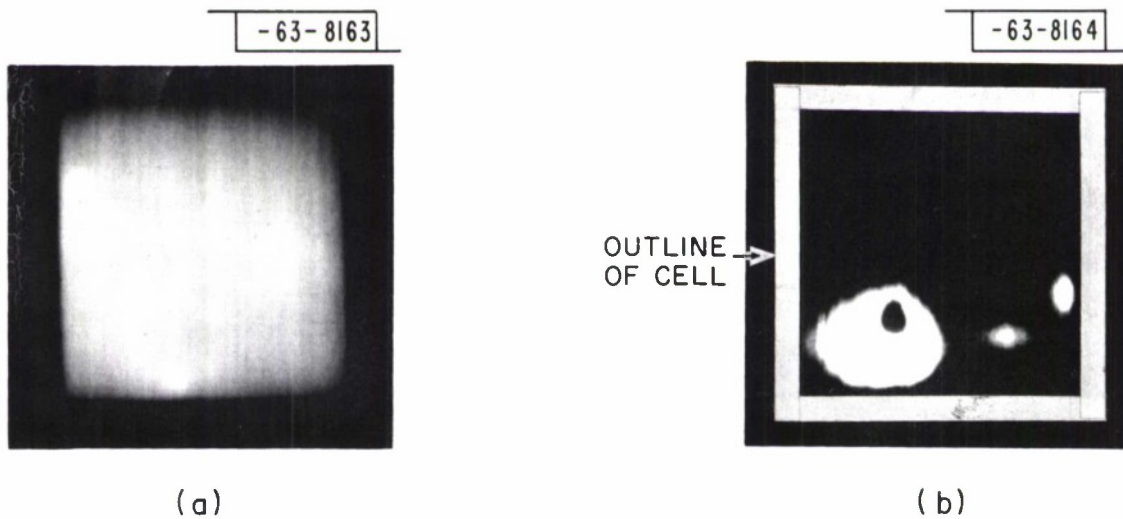


Fig. 9. Infrared thermographs of cadmium sulfide thin-film solar cells; 1A d.c. in forward direction. (a) Standard cell before cycling; dynamic temp. range 1.5°C. (b) Cell without Au-epoxy bond; dynamic temp. range 110°C.

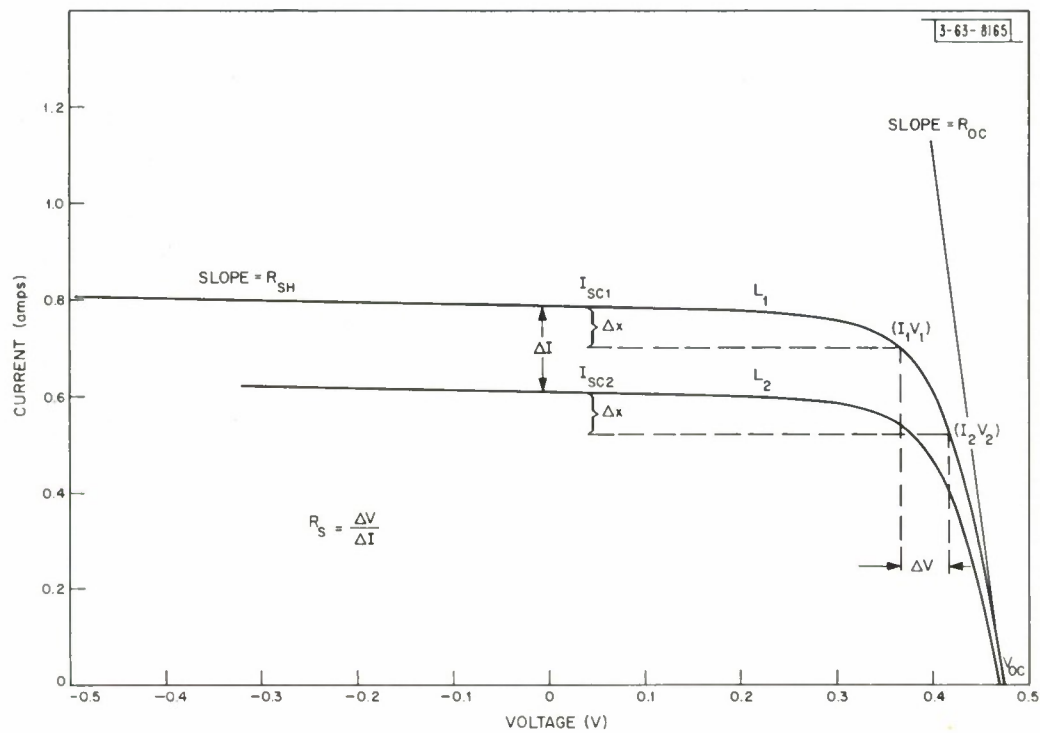


Fig. 10. Measurement of series and shunt resistance.

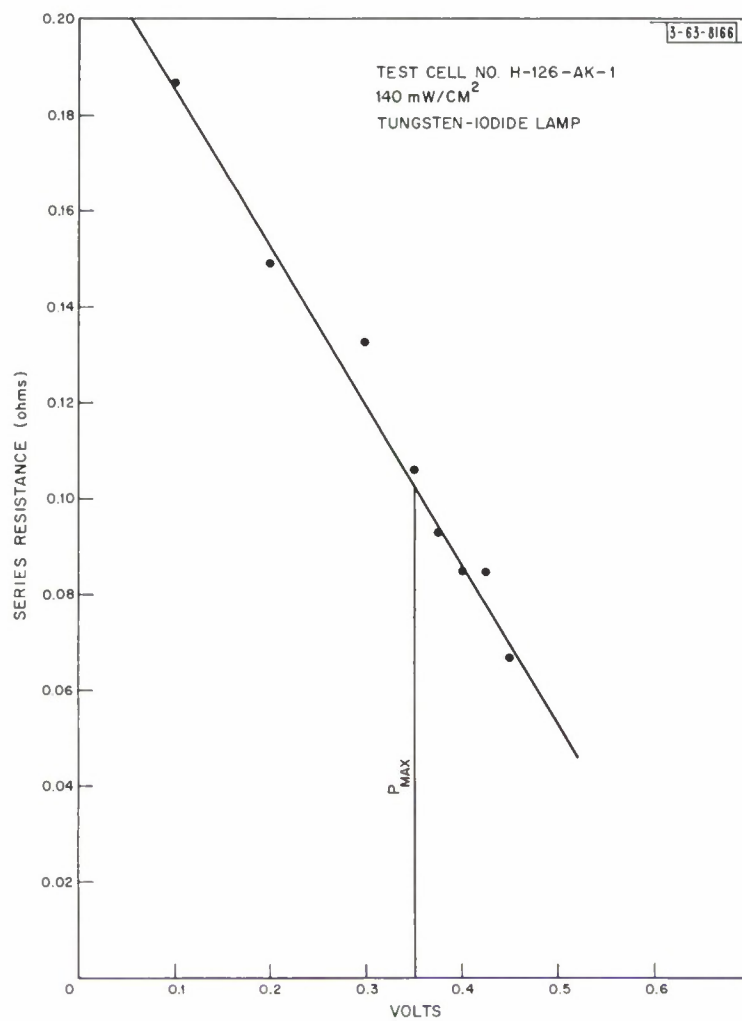


Fig. 11. Series resistance vs. voltage.

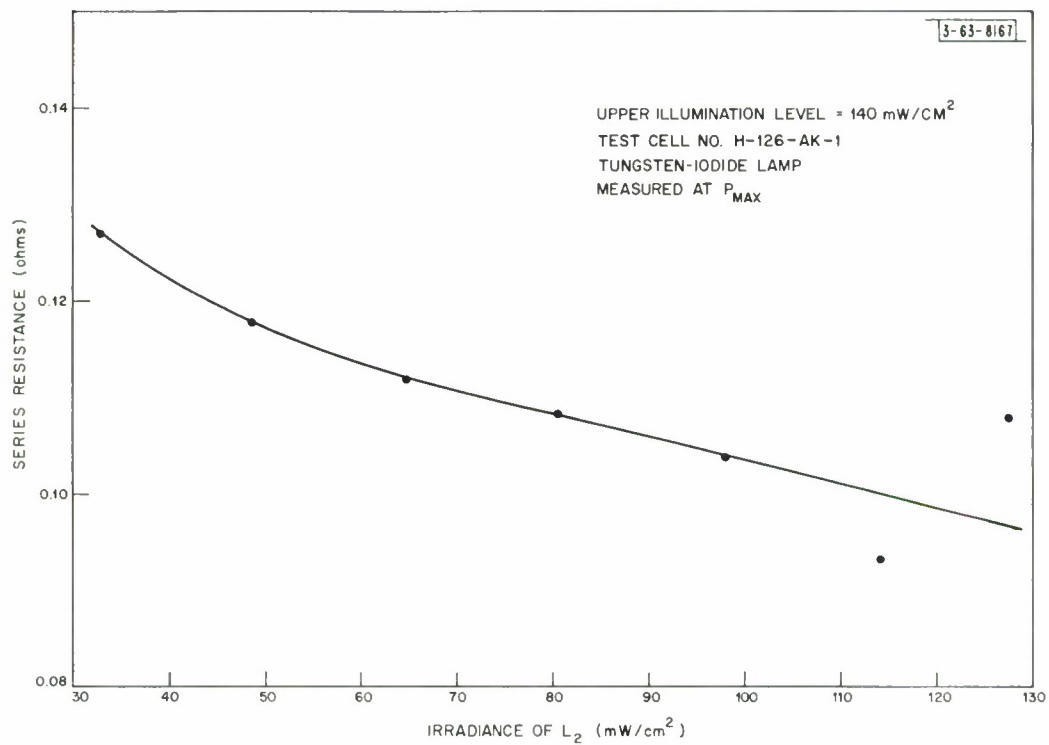


Fig. 12. Series resistance vs. irradiance of lower illumination level  $L_2$ .

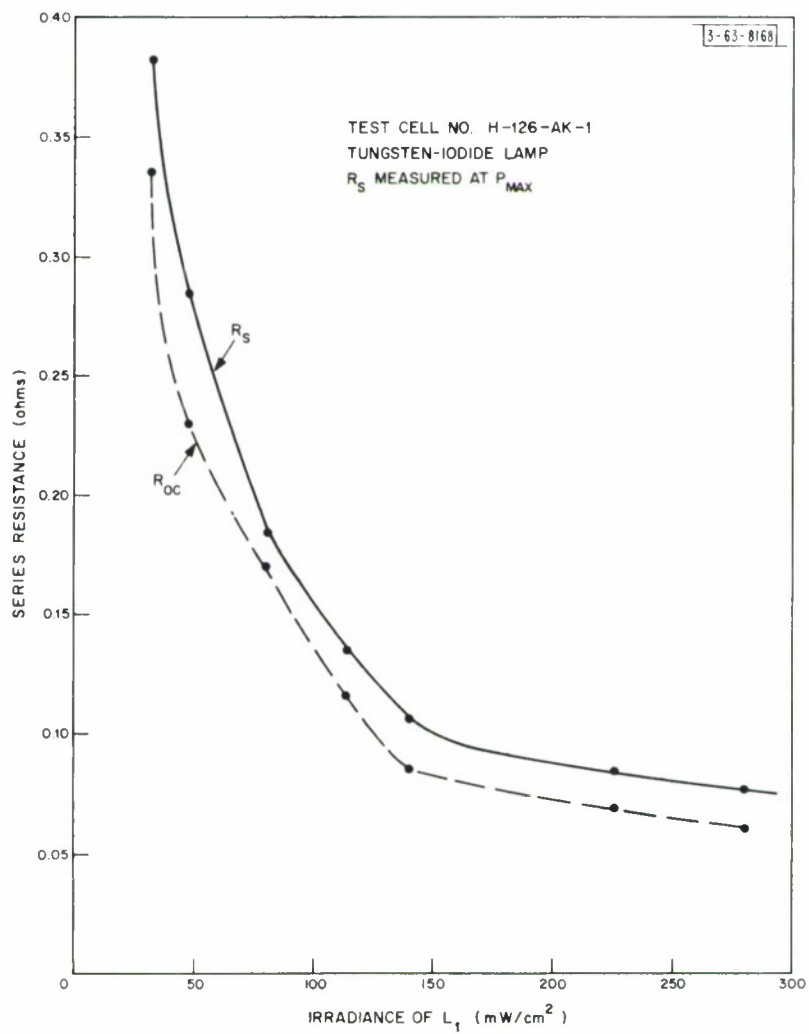


Fig. 13. Series resistance vs. irradiance of  $L_1$ .

DOCUMENT CONTROL DATA - R&D		
<i>(Security classification of title, body of abstract and indexing annotation must be entered when the overall report is classified)</i>		
1. ORIGINATING ACTIVITY (Corporate author)  Lincoln Laboratory, M.I.T.		2a. REPORT SECURITY CLASSIFICATION Unclassified
		2b. GROUP None
3. REPORT TITLE  Present Status of Cadmium Sulfide Thin Film Solar Cells		
4. DESCRIPTIVE NOTES (Type of report and inclusive dates) Technical Note		
5. AUTHOR(S) (Last name, first name, initial)  Stanley, Alan G.		
6. REPORT DATE 13 December 1967	7a. TOTAL NO. OF PAGES 40	7b. NO. OF REFS 19
8a. CONTRACT OR GRANT NO. AF 19 (628)-5167	9a. ORIGINATOR'S REPORT NUMBER(S) Technical Note 1967-52	
b. PROJECT NO. 649L		
c.	9b. OTHER REPORT NO(S) (Any other numbers that may be assigned this report)	
d.	ESD-TR-67-574	
10. AVAILABILITY/LIMITATION NOTICES  This document has been approved for public release and sale; its distribution is unlimited.		
11. SUPPLEMENTARY NOTES  None	12. SPONSORING MILITARY ACTIVITY  Air Force Systems Command, USAF	
13. ABSTRACT  Cadmium sulfide thin film solar cells, specially selected for stability under ambient conditions, experienced severe degradation in their I-V characteristics when subjected to thermal cycling in vacuum. A number of diagnostic techniques were applied to determine the failure mechanism. These included cross-sectioning, infrared measurements, mechanical stress tests and the measurement of series and shunt resistance. Different types of failure modes are discussed. The results of radiation experiments are summarized.		
14. KEY WORDS  cadmium sulfide thin films solar cells		
cross sectioning infrared measurements		
stresses resistance		